Electrochimica Acta 65 (2012) 149–152

Contents lists available at SciVerse ScienceDirect

Electrochimica Acta

journal homepage: www.elsevier.com/locate/electacta

# Preparation and characterization of a novel nickel–palladium electrode supported by silicon nanowires for direct glucose fuel cell

Bairui Tao [a,*], Fengjuan Miao [a], Paul K. Chu [b]

[a] College of Communications and Electronics Engineering, Qiqihar University, 42 Wenhua Street, Qiqihar, Heilongjiang 161006, China
[b] Department of Physics and Material Sciences, City University of Hong Kong, Tat Chee Avenue, Kowloon, Hong Kong, China

ARTICLE INFO

*Article history:*
Received 26 September 2011
Received in revised form 8 January 2012
Accepted 8 January 2012
Available online 16 January 2012

*Keywords:*
Fuel cell
Electrode
Ni–Pd/SiNWs
Ordered array
Alkaline solution

ABSTRACT

Nickel–palladium and silicon nanowires (SiNWs) fabricated by chemical etching and electroless plating (EP) are evaluated as anodes in glucose fuel cells (FC). The effects of processing parameters and structural characteristics such as concentrations of KOH and glucose, medium temperature, and palladium electroless plating on the FC performance are determined. The nickel/silicon electrode exhibits significant activity even without the palladium catalyst and noticeable improvement is observed by incorporating SiNWs. The ordered channels in the SiNWs and coherence rendered by Ni–Pd are important to the enhanced electrode activity. The glucose oxidation current measured from the Ni–Pd/SiNWs electrode is approximately 4.8 mA higher than that on the Ni–Pd/Si one. Our results reveal superior electrooxidation performance and long-term stability and Ni–Pd/SiNWs are useful glucose FC anodes in integrated fuel cell applications.



## 1. Introduction

Direct glucose fuel cells (DGFCs) have attracted much attention as renewable energy sources since glucose is abundant in nature, non-toxic, nonexplosive, and nonvolatile. Furthermore, they can be mass produced and have a relatively high energy content (theoretical energy density of 4430 W h $kg^{-1}$ based on complete oxidation to $CO_2$ via 24-electron transfer) [1–5]. Hence, extensive research is conducted on glucose electrooxidation and associated development of DGFCs [6–8]. Studies on microbial and enzymatic glucose fuel cells are also quite prevalent [9,10], but the low current density, short life-time, poor stability, high cost, and immobilization of bio-catalysts on the electrodes are critical barriers to commercial applications of DGFCs. Noble metal catalysts may enhance the long-term stability and biocompatibility. Although Pt electrodes are widely used in the electrooxidation of glucose, serious poisoning effects introduced by absorbed intermediates, low sensitivity, and poor selectivity act as drawbacks [11]. Hence, identification of better catalysts is vital to the development of DGFCs. The kinetics of glucose oxidation on a metallic electrode depends strongly on the effective surface area [12] and it has also been demonstrated that in alkaline media, the glucose oxidation reaction (GOR) and oxygen reduction reaction (ORR) are enhanced compared to those under acidic and neutral conditions [13–15,8,16,17]. In alkaline DGFCs, metals such as Ag, Au, and Bi [18,19] can be used as the electrode catalysts and $OH^-$ ions in the electrolyte can expedite the kinetics in the ORR.

The main materials (substrate) requirements are large surface area, electrical conductivity, suitable porosity for reactant flux, and stability during the FC operation. The application of three-dimensional materials to the design of FC is an active research area. For instance, silicon nanowires (SiNWs) are a promising substrate with excellent characteristics such as large surface area, relatively high mechanical stability, low cost, and compatibility to commercial microfabrication processes and microelectronics technology. Here, an ordered SiNWs structure is employed as the electrode backbone and Ni–Pd nanoparticle catalysts are electroless-plated on the sidewalls of the SiNWs. This ordered porous electrode exhibits very negative onset potential and strong current response to glucose even in the long-term oxidation of glucose. The excellent performance suggests the feasibility of this composite electrode in nonenzyme glucose catalysis.

## 2. Experimental details

A 100-mm single polished ⟨1 0 0⟩ silicon wafer with a resistivity 2–8 Ω cm and thickness of 525 μm was used as the substrate to fabricate the SiNWs. $NH_4F$, $NiSO_4{\cdot}6H_2O$, $PdCl_2$, $(NH_4)_2SO_4$, HF, $AgNO_3$, sodium citrate, ammonia, glucose, and other chemical reagents were all analytical grade and used without further purification. The solution was prepared with >18 MΩ deionized water and all the experiments were conducted at ~25 °C and 1 atm.

* Corresponding author. Tel.: +86 452 2742787; fax: +86 452 2738748.
*E-mail address:* tbr_sir@163.com (B. Tao).

0013-4686/$ – see front matter © 2012 Elsevier Ltd. All rights reserved.
doi:10.1016/j.electacta.2012.01.017

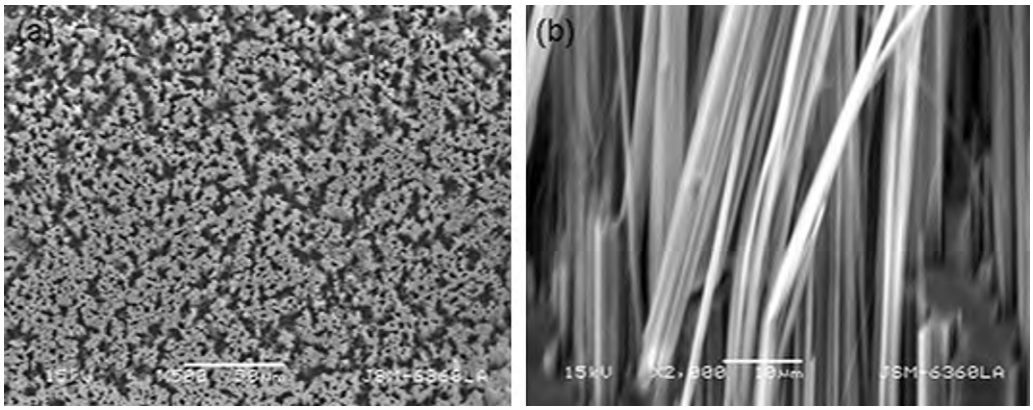


**Fig. 1.** (a) SEM image of the microstructure of the SiNWs and (b) magnified pictures of the cross-sectional SEM images of the microstructure.

The silicon wafer was cleaned using a standard microelectronics process and cut into 1 cm × 1 cm pieces. Before fabrication of the SiNWs, the unpolished side was protected by photoresist and used for marking the electrode pad. The silicon nanowires were synthesized by chemical etching based on the procedures described in Refs. [20,21]. A solution [HF (20%): $AgNO_3$ (35 mM) = 1:1 (v/v)] was used as the etchant and after the formation of SiNWs, the silicon pieces were removed from the solution and rinsed with DI water and diluted nitric acid (∼30%) to remove surface residues.

Prior to electrodeposition of the Ni–Pd nanoparticles, the SiNWs were dipped in a solution of Triton X-100 30 s to decrease the internal stress and enhance wetting. A thin nickel film was coated on the SiNWs by electroless plating to serve as the electrically conductive layer and to obtain better resistance against alkaline media. More details about the Ni electroless plating process can be found in Ref. [22]. The Pd nanoparticles were produced on the sidewall of the SiNWs by electroplating. The Ni/SiNWs sample was dipped in the electroplating solution [23]. $PdCl_2$ was used as the metal source and EDTA as the complexing agent. The plating bath was kept at 60 °C and rigorously stirred. The pH value of the bath was kept at 8.0–9.0 by adding ammonia and the current density was 50 mA $cm^{-2}$ [22]. The Ni–Pd/SiNWs were then rapid thermal annealed at 400 °C in argon. Copper wires were connected to the silver conductive adhesive for the subsequent electrochemical experiments.

The surface morphology and structure were assessed by scanning electron microscopy (SEM, JSM 5610) at an accelerating voltage of 10 kV and the deposited materials were characterized by XRD (X-ray diffraction) using Cu $K_\alpha$ radiation. The electrochemical properties of the Ni–Pd/SiNWs were determined by cyclic voltammetry (CV) and chronoamperometric technique. The electrochemical experiments were performed on a LK3200A electrochemical workstation (Tianjin, China). The modified SiNWs served as the working electrode and a platinum wire formed the counter electrode. All the potentials were referenced to the SCE reference electrode.

## 3. Results and discussion

Fig. 1 depicts the top-view (a) and cross-sectional (b) images of the SiNWs before electroless plating. The SiNWs have a bundled morphology and are aligned vertically to the substrate. The interface between the SiNWs and bulk silicon is clear and layered. The length of the SiNWs is uniform and about 90 μm, which can be controlled by choosing a different etching time. The diameters of the SiNWs vary between 60 and 300 nm. The structure has good surface quality and provides more effective surface area than a planar electrode. Fig. 2(a) shows the surface topography of the cross-section of the Ni–Pd/SiNWs structure. An additional thin layer of Ni–Pd nanoparticles can be observed on the SiNWs. The diameter of the Pd

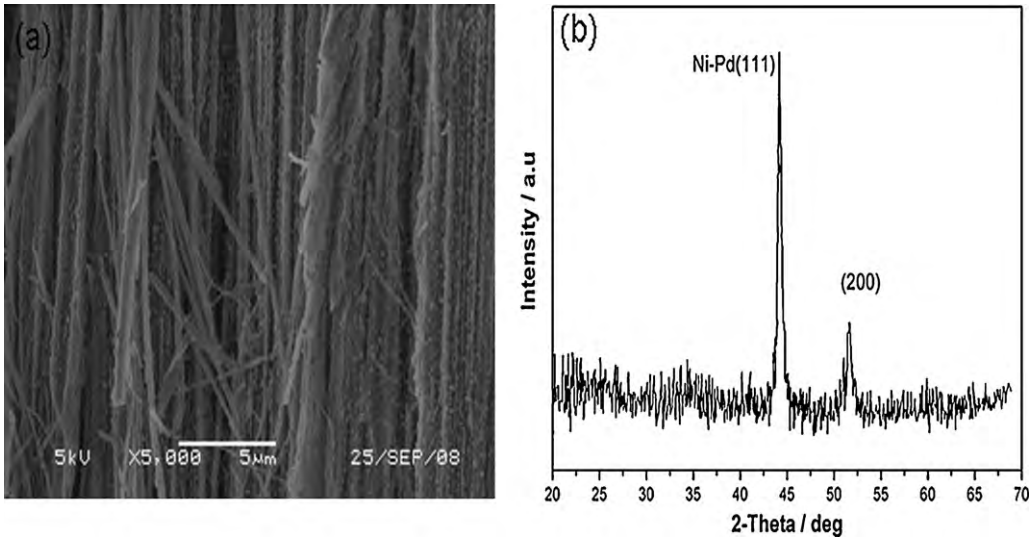


**Fig. 2.** (a) Cross-sectional SEM image of the Ni–Pd/SiNWs after electroplating nickel–palladium and (b) X-ray diffraction pattern of the Ni–Pd/SiNWs electrode.

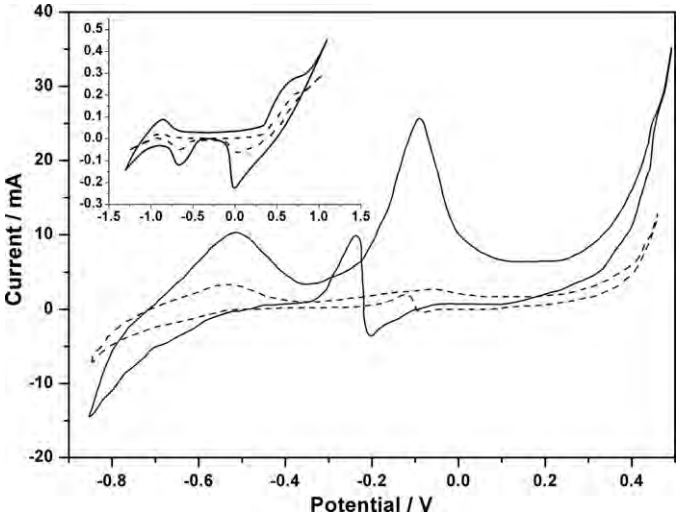


**Fig. 3.** Cyclic voltammograms of the Ni–Pd/SiNWs (solid curve) electrode and Ni–Pd/Si (dashed curve) in the absence (inset of Fig. 3) and presence of 1 M glucose in a 1.0 M KOH solution at a scanning rate of 50 mV $s^{-1}$.

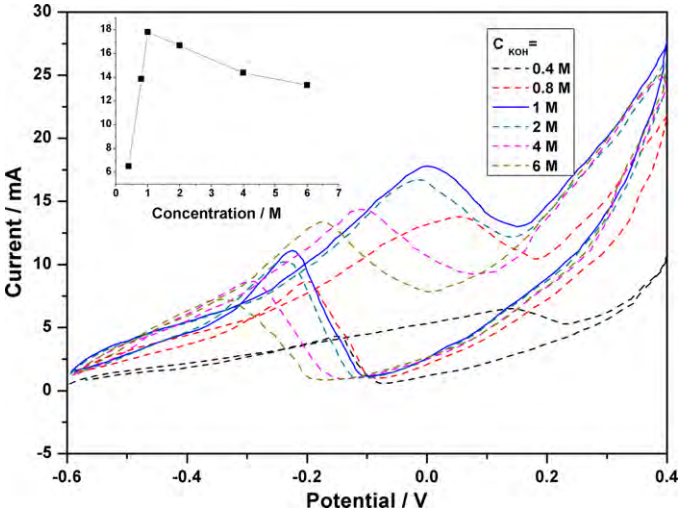


**Fig. 4.** Cyclic voltammograms of the 1 M glucose oxidation reaction on the Ni–Pd/SiNWs electrode at various concentrations of KOH and the variations of the anodic peak current for glucose electrooxidation versus KOH concentrations on the Ni–Pd/SiNWs electrode in the inset of Fig. 4 at a potential scanning rate of 50 mV $s^{-1}$.

and Ni particles ranges from tens to hundreds of nanometer and the palladium and nickel particles cover the entire silicon nanowires even at the bottom. The structure is characterized by X-ray diffraction (XRD). Fig. 2(b) shows the representative XRD patterns of the sample annealed at 400 °C. Two peaks emerge from the pattern of Ni–Pd/SiNWs at 44.12° and 51.66°. The former is the characteristic peak of Ni (1 1 1) with a slight shift and the peak at 51.66° is ascribed to the Pd (2 0 0) plane. The results confirm the Ni–Pd structure.

The electrocatalytic activity of the Ni–Pd/SiNWs electrode towards glucose oxidation under alkaline conditions is investigated by cyclic voltammetry and chronoamperometric technique. Fig. 3 displays the electrochemical response of Ni–Pd/Si (dashed curve) and Ni–Pd/SiNWs electrodes in a 1 M KOH solution containing 1 M glucose measured at a scanning rate of 50 mV $s^{-1}$. The cyclic voltammograms of the Ni–Pd/SiNWs (solid curve) and Ni–Pd/Si (dashed curve) electrodes in 1 M KOH in the absence of glucose are shown in the insets of Fig. 3. The oxidation or reduction peaks can be observed and the current density of the Ni–Pd/SiNWs is clearly greater than that of the Ni–Pd/Si implying that the two electrodes have catalytic capability and the Ni–Pd/SiNWs have higher catalytic activity. The hydrogen adsorption/desorption peaks are observed at a negative potential region due to oxidation of hydrogen adsorbed on the metal. In the positive scan, Ni–Pd adsorbs $OH^-$ and an inactive oxide film is formed on the electrodes. The two reduction peaks are found at potentials of −0.66 V and 0 V and they arise from reduction of $Ni^{2+}$ or $Ni^{3+}$ and reduction of $Pd^{2+}$, respectively [23–25].

In the presence of 1 M glucose, electrooxidation is characterized by two well-defined current peaks in the forward and reverse scans. An oxidative peak in the anodic scan is mainly attributed to the electrocatalytic oxidation of glucose by the Pd nanoparticles. The reoxidation peak is primarily associated with the removal of incompletely oxidized species formed in the forward scan [26]. The current densities are higher at the corresponding potentials on the Ni–Pd/SiNWs electrode compared to the Ni–Pd/Si electrode. The results suggest that Ni–Pd nanoparticles have superior electrocatalytic activity towards glucose oxidation in an alkaline solution, and the Ni–Pd/SiNWs electrode has much higher catalytic activity for glucose electrooxidation than Ni–Pd/Si under alkaline conditions.

The effect of different KOH concentrations (0.4–6 M) on the Ni–Pd/SiNWs electrode in 1 M glucose is investigated by CV. Fig. 4 shows the CVs in 1 M glucose solution from −0.6 to 0.4 V. The oxidation current increases as the KOH concentration is increased from 0.4 to 1 M and further increase leads to an obvious decrease in the peak current. Furthermore, the peak potential shows a continuous negative-shift similar to that of glucose oxidation.

At first the glucose oxidation reaction on the Ni–Pd/SiNWs electrode is accelerated at higher $OH^-$ concentrations. This increases the anodic peak current, but at higher KOH concentrations, adsorption of hydroxyl ions may be dominant on the Ni–Pd/SiNWs electrode and it blocks adsorption of glucose onto the electrode. The imbalance reduces the anodic peak current [26]. The relationship between the KOH concentration and peak current in the forward scan is shown in the inset of Fig. 4.

The CVs of the Ni–Pd/SiNWs electrode in the glucose solutions with different concentrations from 0.5 to 2.5 M in 1 M KOH solution are displayed in Fig. 5. The oxidation current increases monotonically with glucose concentration. Furthermore, the peak potential shows a continuous positive-shift as the glucose concentration is increased. It appears that at a lower glucose concentration, the glucose concentration and coverage of $OH^-$ are independent of each other. As the glucose concentration is increased, adsorption of glucose onto the electrode becomes dominant and adsorption of

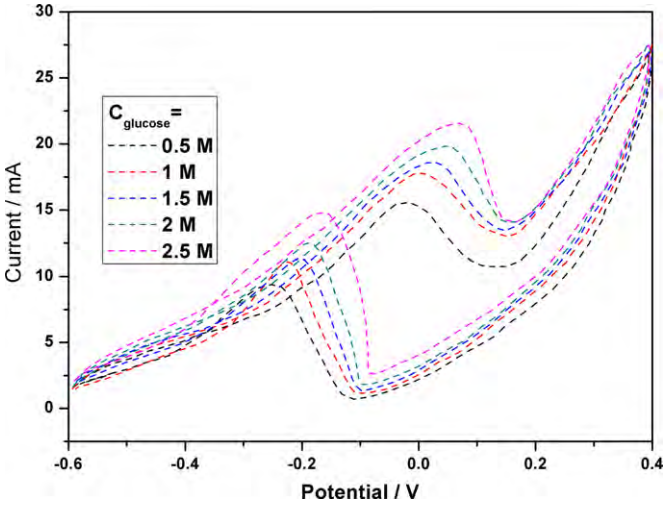


**Fig. 5.** Cyclic voltammograms of the glucose oxidation reaction on the Ni–Pd/SiNWs electrode in 1 M KOH solution containing glucose of various concentrations at a scanning rate of 50 mV $s^{-1}$.

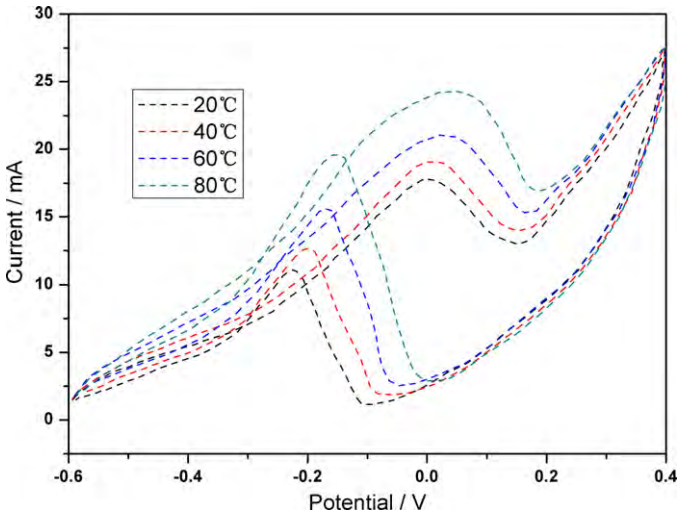


**Fig. 6.** Cyclic voltammograms of the Ni–Pd/SiNWs in 1 M KOH containing 1 M glucose at various temperatures at a potential scanning rate of 50 mV $s^{-1}$.

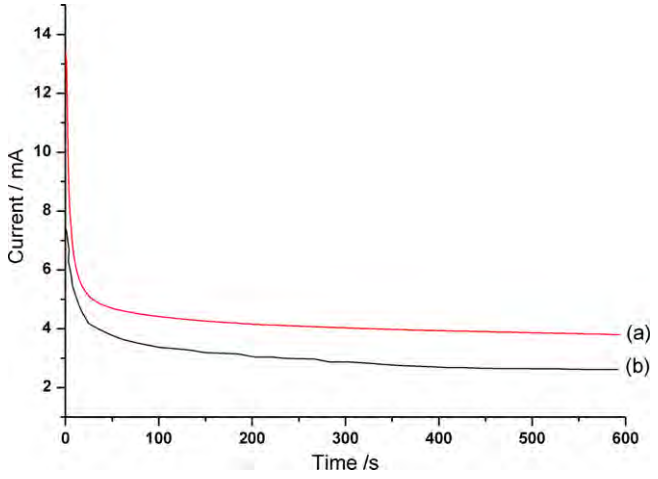


**Fig. 7.** Chronoamperogram of electroactivity of (a) Ni–Pd/SiNWs and (b) Ni–Pd/Si electrode at an oxidation potential −0.4 V for glucose electrooxidation in 2 M KOH and 1 M glucose solution at 25 °C.

hydroxyl ions is blocked, thereby leading to reduced anodic peak current.

The effect of the medium temperature on electrooxidation of glucose is investigated. Fig. 6 depicts the CV of the Ni–Pd/SiNWs electrode during glucose oxidation at different temperatures. A higher temperature increases the anodic peak current but the rate is nonlinear. Some other special characteristics are also observed, such as a positive shift in the anodic oxidation and re-oxidation peak potential and a negative shift in the onset potential. As the temperature is increased, the difference in the onset potentials becomes smaller and a higher temperature facilitates electrooxidation of glucose.

The chronoamperometric technique is an effective method to evaluate the electrocatalytic activity and stability of catalysts. Fig. 7 shows the chronoamperogram of the electroactivity of the Ni–Pd/SiNWs (a) and Ni–Pd/Si (b) electrodes at an oxidation potential –0.1 V in 1 M KOH/1 M glucose at 25 °C. As expected, the glucose oxidation current on the Ni–Pd/SiNWs electrode is evidently higher than that on the Ni–Pd/Si. The chronoamperogram also shows that electrocatalytic oxidation of glucose is maintained at high activity and is very stable for over 600 s. This provides the evidence that most CO species can be oxidized and removed from the Ni–Pd catalysts and our results indicate that the Ni–Pd/SiNWs nanocomposites have the better electrocatalytic properties.

## 4. Conclusion

A glucose fuel cell prototype is fabricated by electrodeposition plating Ni–Pd nanoparticles on ordered aligned Si nanowires arrays. The Ni–Pd/SiNWs electrode possesses many desirable features such as high electrocatalytic activity and good stability due to the large effective surface area and electrocatalytic activity of Ni–Pd nanoparticles. The Ni–Pd/SiNWs electrode is attractive in direct glucose fuel cell.

## Acknowledgments

This work was jointly supported by Natural Science Foundation of Heilongjiang Province (no. F201008 and QC2011C092), Program for Young Teachers Scientific Research in Qiqihar University (Grant no. 2010k-Z02 and 2011k-Z01), Excellent Young Scholars of Higher University of Heilongjiang Province no. 1251G067, Science and Technology Project of Qiqihar, Grant GYGG2010-03-1 and City University of Hong Kong Research Grant 9360110.

## References

[1] S.K. Chaudhuri, D.R. Lovley, Nat. Biotechnol. 21 (2003) 1229–1232.
[2] J. Ryu, H.-S. Kimb, H. Thomas, D. Lashmore, Biosens. Bioelectron. 25 (2010) 1603.
[3] S. Kerzenmacher, J. Ducree, R. Zengerle, F. von Stetten, J. Power Sources 182 (2008) 66.
[4] N. Fujiwara, S. Yamazaki, Z. Siroma, T. Ioroi, H. Senoh, K. Yasuda, Electrochem. Commun. 11 (2009) 390.
[5] S. Kerzenmacher, J. Ducree, R. Zengerle, F. von Stetten, J. Power Sources 182 (2008) 1.
[6] L.H. Li, W.D. Zhang, J.S. Ye, Electroanalysis 20 (2008) 2212.
[7] F. Xiao, F. Zhao, D. Mei, Z. Mo, B. Zeng, Biosens. Bioelectron. 24 (2009) 3481.
[8] H.F. Cui, J.S. Ye, X. Liu, W.D. Zhang, F.S. Sheu, Nanotechnology 17 (2006) 2334.
[9] V. Soukharev, N. Mano, A. Heller, J. Am. Chem. Soc. 126 (2004) 8368.
[10] P. Kavanagh, S. Boland, P. Jenkins, D. Leech, Fuel Cells 9 (2009) 79.
[11] Z. Liua, L. Huangb, L. Zhanga, H. Maa, Y. Dinga, Electrochim. Acta 54 (2009) 7286.
[12] Y. Chen, W. Schuhmann, A.W. Hassel, Electrochem. Commun. 11 (2009) 2036.
[13] H.F. Cui, J.S. Ye, X. Liu, D.W. Zhang, F.S. Sheu, Nanotechnology 17 (2006) 2334–2339.
[14] J. McGinley, F.N. McHale, P. Hughes, C.N. Reid, A.P. McHale, Biotechnol. Lett. 26 (2004) 1771.
[15] D. Basu, S. Basu, Electrochim. Acta 55 (2010) 5775.
[16] M. Besson, P. Gallezot, Catal. Today 57 (2000) 127.
[17] C.P. Wilde, M. Zhang, J. Chem. Soc. Faraday Trans. 89 (1993) 385.
[18] Z.N. Liu, L.H. Huang, L.L. Zhang, H.Y. Ma, Y. Ding, Electrochim. Acta 54 (2009) 7286–7293.
[19] D. Basu, S. Basu, Electrochim. Acta 56 (2011) 6106–6113.
[20] B.R. Tao, J. Zhang, S.C. Hui, L.J. Wan, Sens. Actuators, B 142 (2009) 298–303.
[21] F.J. Miao, B.R. Tao, L. Sun, T. Liu, J.C. You, L.W. Wang, P.K. Chu, Sens. Actuators, A 160 (2010) 48–53.
[22] J. Shi, P.L. Ci, F. Wang, H. Peng, P.X. Yang, L.W. Wang, Electrochim. Acta 56 (2011) 4197–4202.
[23] Y.Y. Liao, T.C. Chou, Electroanalysis 12 (2000) 55.
[24] Y.L. Lo, B.J. Hwang, Langmuir 14 (1998) 944.
[25] J. Munk, P.A. Christensen, A. Hammnett, E. Skou, J. Electroanal. Chem. 401 (1996) 215.
[26] Z.X. Liang, T.S. Zhao, J.B. Xu, L.D. Zhu, Electrochim. Acta 54 (2009) 2203.